Available online at www.sciencedirect.com
SCIENCE DIRECT®
Journal of Electroanalytical Chemistry 565 (2004) 21–28
Journal of Electroanalytical Chemistry
www.elsevier.com/locate/jelechem

The electrochemical characteristics of blue copper protein monolayers on gold

L. Andolfi [a], D. Bruce [b], S. Cannistraro [a], G.W. Canters [c], J.J. Davis [b,*], H.A.O. Hill [b], J. Crozier [b], M.Ph. Verbeet [c], C.L. Wrathmell [b], Y. Astier [b]

[a] *Unita INFM Dipartmento di Scienze Ambientali, Universita della Tuscia, I-01100 Viterbo, Italy*
[b] *Inorganic Chemistry Laboratory, University of Oxford, Oxford OX1 3QR, UK*
[c] *Leiden Institute of Chemistry, Gorlaeus Laboratoria, Leiden University, Leiden, The Netherlands*

Received 31 January 2003; received in revised form 22 August 2003; accepted 14 September 2003

Abstract

Site-specifically engineered disulphide or surface cysteine residues have been introduced into two blue copper proteins, *Pseudomonas aeruginosa* azurin and *Populus nigra* plastocyanin, in order to facilitate protein chemisorption on gold electrodes. The subsequently formed well-defined protein monolayers gave rise to robust electrochemical responses and electron transfer rates comparable to those observed at modified electrode surfaces. Proximal probe characterisation confirms the presence, at high coverage, of well-ordered protein adlayers. Additionally, gold-metalloprotein affinity is such that molecular-level tunnelling and topographic analyses can be carried out under aqueous solution. The approaches outlined in this work can, in principal, be extended to the generation of arrays of any redox-active biomolecule.

Keywords: Plastocyanin; Azurin; Protein monolayer; Self-assembly; Copper metalloprotein; Protein tunnelling

1. Introduction

Metalloprotein electrochemical studies have led, not only to an enhanced understanding of the important role these molecules play in biological energy transduction processes (including structure/function correlations) but also to significant biosensing developments and, more recently, the birth of bioelectronics. Much progress has been made during the past 20 years in attaining reproducible electrochemical responses from metalloproteins and enzymes [1]. Particularly beneficial in this context is the level of control achievable by confining voltammetric investigations to the electrode surface (and thereby removing complicating diffusion-based contributions to voltammetry) [2,3]. The process of electron exchange between planar electrode surfaces and immobilised metalloproteins has now advanced to the point where detailed kinetic and thermodynamic investigations, including quantitative electronic coupling (such as structure and distance dependence) experiments and reorganisation can be pursued [2,4]. Controlling the electrochemical coupling between biomolecules and man-made circuitry is, further, of considerable importance in the development of improved bio- and immunosensing devices.

Reliable (that is, reproducible) heterogeneous electron transfer of metalloproteins at man-made electrode surfaces is achievable only through careful consideration of protein and electrode surface chemistry [5–7]. Specifically, much work has centered on ''modelling'' the electrode surface such that its physiochemical interactions with the protein reflect, to variant levels of simplification, the natural interfacial interactions of the protein in its native environment. Indeed, the force balance imposed on a metalloprotein confined to an electrode surface differs from that in solution and this commonly leads to a loss of native conformation unless specific steps are taken to create a ''biocompatible

* Corresponding author. Tel.: +44-1865-275-914; fax: +44-1865-275-914.
E-mail address: jason.davis@chem.ox.ac.uk (J.J. Davis).

0022-0728/$ - see front matter © 2003 Elsevier B.V. All rights reserved.
doi:10.1016/j.jelechem.2003.09.038

interface'' [8]. Much success has been obtained at modified noble metal surfaces (particularly gold and silver) through the use of surface self-assembly [8]; typically, one tailors the electrode interface such that its interactions with the solution-phase protein model, as much as is possible, the natural protein–protein or protein–membrane interfacial interactions prevalent in biology. Significantly in the context of this work, though metalloproteins have been observed to exchange electrons with bare metal surfaces, these responses are usually both transient and poorly reproducible [9,10]. In recent years, we, and others, have developed methods whereby metalloproteins can be assembled on electrode surfaces in well-defined, electrochemically addressable, molecular arrays [11–15]. We have specifically made use of the introduction of thiol-terminating cysteine residues into the surface of metalloproteins as a means of tethering them controllably to gold electrode surfaces. This methodology is demonstrably successful in producing well-defined, mechanically robust, molecular arrays suitable for molecular-level electronic analysis [13,14].

The plastocyanins (PC) are small (9–14 kDa) mononuclear type-1 copper proteins, characterised by an intense absorption band in the visible spectrum (~600 nm). They belong to the cupredoxin family and function as electron carriers in the photosynthetic chains of plants, algae and cyanobacteria [16]. In plants, the proteins are located in the thylakoid lumen of the chloroplast, where they are reduced by cytochrome *f* and oxidised by the P700 reaction centre of photosystem I (PSI) (ultimately shuttling electrons from PSII to PSI). High-resolution crystal and/or NMR structures have been obtained from, amongst others, poplar [17], *Oleander nerium* [18], French bean [19], spinach [20] and parsley [21]. In this class of blue copper proteins, the redox-active (Cu^{II}–Cu^{I}) copper centre is strongly coordinated by the sulphur of a cysteine and the nitrogens of two histidine residues. In most type-1 sites, including those of plastocyanin, the sulphur of a methionine moiety provides a point of fourth ligation. Characteristically, the copper site geometry is largely conserved across the two oxidation states and, consequently, the inner-sphere re-organisational energy associated with electron transfer, is low [22,23]. The poplar protein (*Populus nigra*), a 99-amino-acid, eight-stranded antiparallel β-sheet, bears a net negative charge at pH 7.0 [24]. When looking at the protein as it is commonly depicted in the literature, the redox site at the ''northern pole'' of the molecule is in the vicinity of the ''hydrophobic'' interaction patch and ''west'' of the negatively charged interaction patch [25]. Site-directed mutagenesis has been recently used to modify both the copper ligation and interaction patches [26]. In this work, a site-specifically engineered disulphide bridge, located in a region of the poplar plastocyanin structure opposite to the copper active site, was introduced [27,28]. Such a mutation (PCSS) was aimed at achieving a stable and redox-active protein able to self-assemble on gold surfaces. Following the binding of the PC via the disulphide bridge the copper centre should be some 3 nm from the metal surface. The redox activity of self-assembled PCSS was further compared with immobilised wild-type plastocyanin in which this anchoring group is absent.

Azurin is a well-characterised blue copper protein involved in bacterial electron transfer chains, such as those in *Pseudomonas aeruginosa* [29]. Though the wild-type form of azurin can be immobilized on pristine gold electrode surfaces through its exposed disulphide moiety, previous studies have reported that such arrays are electrochemically inactive [14]. As with plastocyanin, we have sought to control protein–electrode mechanical and electronic coupling through the use of site-selective mutagenesis. With both proteins, the designed introduction of gold-anchoring cysteine residues into the surface of the protein is achieved without significant structural/functional perturbation of the wild-type structure.

2. Experimental

2.1. Mutagenesis, protein purification and expression

The S118C and K27C azurin mutants (*P. aeruginosa*) were isolated under reducing conditions in their apo forms as has been previously described [30]. The holo proteins were typically formed through the addition of 1.1 molar equivalents of $Cu(NO_3)_2$ solution and an excess (4–5 molar equivalents) of $K_3[Fe(CN)_6]$. Gel filtration chromatography (Superdex 75, Pharmacia) was used to purify the monomer from dimeric forms.

Reagents and gene mutation details for plastocyanin have been published [27]. Briefly, wild-type and PCSS mutants were expressed in *Escherichia coli* HMS174 (DE3) and released from the bacterial cells by freeze–thaw cycling. The supernatant resulting from centrifugation was dialysed against 0.5 mM $MgCl_2$ and then a batch-wise binding step using a DEAE Sepharose fast-flow column (Pharmacia) was performed; subsequently, the protein was eluted with 20 mM sodium phosphate buffer, pH 6 and 300 mM NaCl. In a second DEAE column chromatography step the PCSS protein was eluted by using a linear salt gradient. As a final purification step, the protein was eluted (20 mM sodium phosphate, pH 6, 150 mM NaCl) through a Superdex 75 size-exclusion column in a Pharmacia FPLC system. Sample purity was verified by SDS–PAGE and an isoelectric focussing gel (PhastGel IEF 3-9 Pharmacia). Further characterisation was carried out by UV–Vis spectroscopy (Perkin–Elmer Lambda 800 and Perkin–Elmer Lambda 20), resonance Raman spectroscopy (Dilor LaBram (ISA)) and electron paramagnetic resonance (X-band Varian E109 spectrometer).

2.2. Protein immobilisation and voltammetric characterisation

Prior to voltammetric experiments, polycrystalline gold electrodes were exhaustively polished with an Al_2O_3 slurry on a polishing cloth (Beuhler) and rinsed with water (18.2 MΩ cm, Elga). They were subsequently further cleaned by electropolishing in 1 M H_2SO_4 (99.9% Sigma) in the range of −0.3 to +1.5 V vs a standard calomel electrode (SCE). Edge plane graphite (EPG) electrodes were mechanically polished. Protein self-assembly was carried out by incubating freshly cleaned (and characterised) gold electrodes in 3–30 μM plastocyanin at 5 °C overnight in 100 mM potassium phosphate buffer, pH 7.4. The electrodes were subsequently rinsed with pure water and characterised.

Voltammetry was carried out using a μ-autolab potentiostat (Ecochemie, Netherlands) and a home-made glass cell with a conventional three electrode two compartment configuration. The counter electrode was a platinum wire gauze and the reference a standard calomel electrode (SCE, Radiometer, UK). The reported potentials are corrected to SHE using a value of 241 mV at 25 °C. All voltammetric experiments were performed in 100 mM potassium phosphate at pH 7.14. Background subtraction in the voltammograms was achieved by using a computer program, obtained from Prof. F.A. Armstrong (University of Oxford), which fits a cubic spline function to the data [2]. For practical reasons, most voltammetry has been performed on polycrystalline gold electrodes. Responses obtained at "single crystal" (evaporated gold film) electrodes displayed the same kinetic and half wave potentials as outlined below for polycrystalline surfaces. Imaging experiments were, necessarily, carried out at atomically flat single crystal surfaces.

2.3. Tunnelling imaging

Atomically flat gold electrode surfaces were prepared by evaporation on to mica at low pressure (ca. 1×10^{-5} mbar) to a thickness ~200 nm then flame annealed using a butane torch. Protein adlayers were prepared by treating a freshly prepared gold surface with high-purity protein of concentration 1–2 μM, leaving to self-assemble overnight at 5 °C. STM experiments were performed in constant current mode using a Molecular Imaging STM (LOT Oriel UK). Tips were prepared from 0.25 mm diameter tungsten wire electrochemically etched in 2 M NaOH and coated in an insulating layer of apiezon wax. Low-temperature imaging was carried out under fluid (50% deionised water + 50% glycerol (BDH)) in conjunction with a triple-stage peltier-cooled cold stage controlled using a Lakeshore Model 330 autotuning temperature controller.

For imaging purposes, plastocyanin adlayers were prepared by incubation of freshly annealed evaporated gold film in 30 μM PCSS in 20 mM sodium phosphate, pH 6.0, for about 1 h at 4 °C. Samples were rinsed with buffer solution, blown dry with pure nitrogen and immediately imaged. The tunnelling set point was 50 pA and the bias 180 mV, scan rate 4 Hz.

2.4. Gold electrode dithiol modification

Freshly annealed evaporated gold films or polished polycrystalline electrode surfaces were soaked in 1–1.5 mM ethanolic solutions of pentanedithiol, 1,6-hexanedithiol, 1,8-octanedithiol or dodecanethiol (Aldrich) overnight at 5 °C. The surfaces were rinsed profusely in ethanol, incubated in 1–3 μM solutions of the protein overnight, washed and analysed. AFM analyses were consistent with minimal penetration of the protein into the dithiol adlayer.

3. Results

Preliminary scanning tunnelling experiments confirmed (Fig. 1) that well-defined molecular adlayers could be formed by exposure of pristine gold surfaces to PCSS; an interaction depicted schematically in Fig. 2. Facile, quasi-reversible, electron transfer has been observed with a number of plastocyanins in diffusive voltammetric studies [31,32]. This interfacial electron transfer has been shown to be highly site-specific, with sigmoidal responses typically observed under conditions

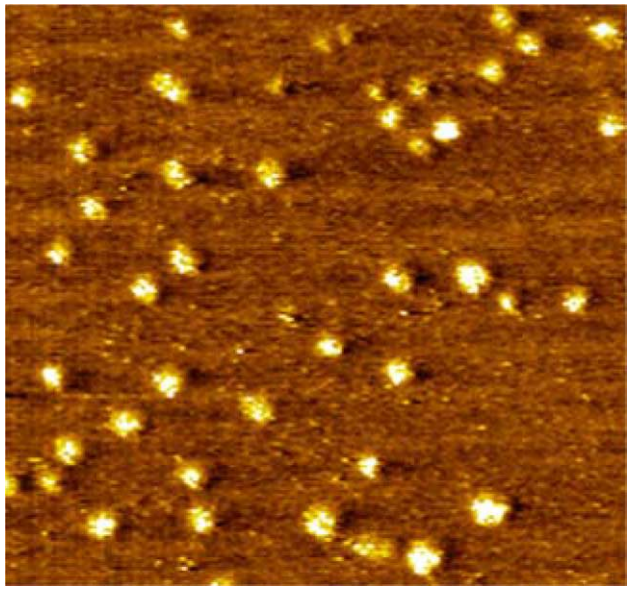

Fig. 1. Ambient tunnelling image of low-coverage of PCSS on Au[III]. Such images were acquired with Pt/Ir probes at a constant tunnelling current of 1 nA (bias 100 mV, tip positive). Image size 180 × 180 nm.

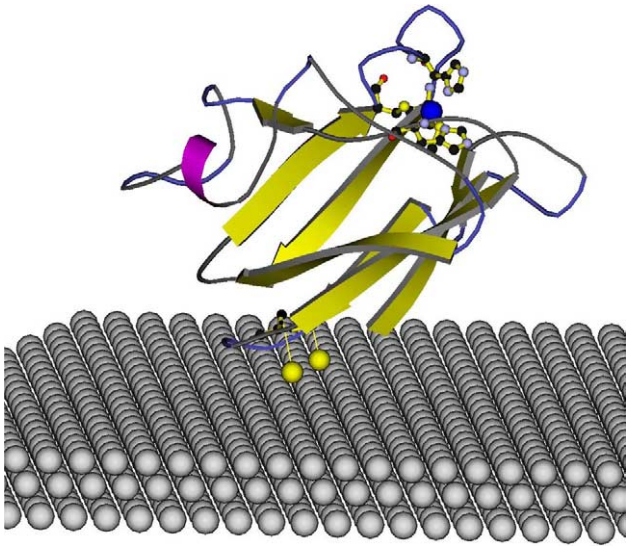

Fig. 2. Graphical representation (Molscript) of the interaction of poplar plastocyanin with an Au[III] surface. This HIS-87, CYS-84, MET-92 and HIS-37 ligation is shown.

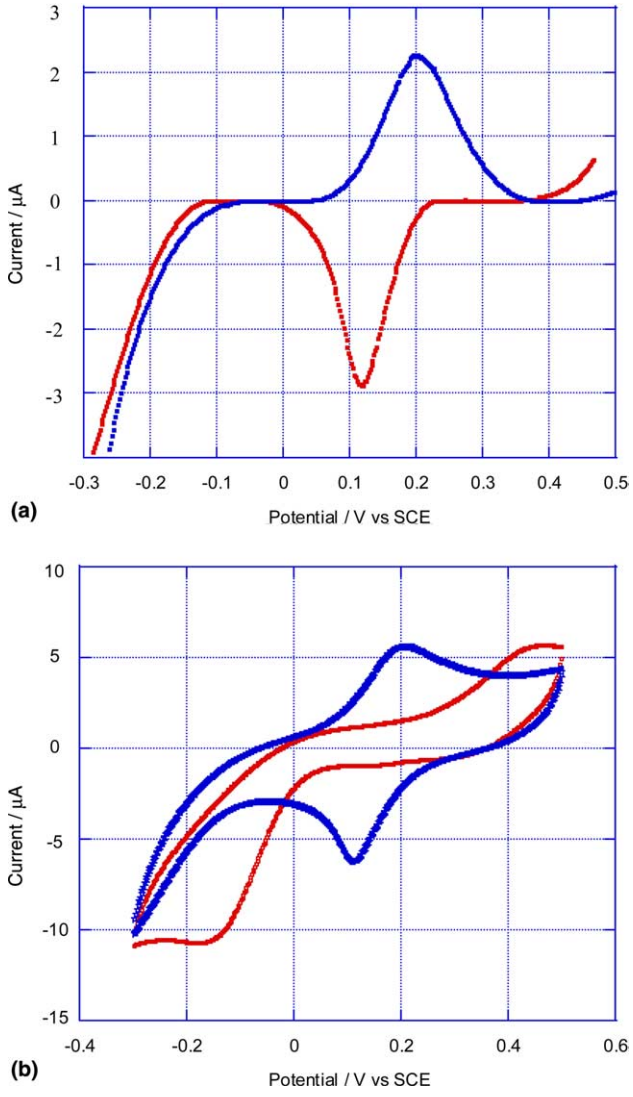

Fig. 3. (a) Background corrected voltammogram recorded for PCSS monolayers at 100 mV s^{-1} scan rate in 100 mM potassium phosphate buffer, pH 7.14. (b) Comparative voltammetry (100 mV s^{-1}) of self-assembled PCWT (*red line*) and PCSS (*blue line*) adlayers. For colour, see on-line figure.

of low surface "binding site" concentration. Robust voltammetric responses, stable to continual (>100 cycles at 10 mV s^{-1}) scanning, were obtained for PCSS adlayers on polycrystalline gold (Figs. 3(a) and (b)). Electroactive surface coverages, estimated by integrating the faradaic responses, and correcting for an AFM-determined surface roughness factor of 1.3, were 2–8×10^{14} molecules cm^{-2} (Table 1). This value is both in good agreement with an expected coverage for a molecule with a lateral dimension of ~3.5 nm and confirmatory of a high degree of structural retention. The redox midpoint potential of the PCSS adlayer was 404 ± 10 mV vs SHE, a value close to that obtained diffusively with the wild-type protein at EPG [33]. This is, again, consistent with immobilisation occurring without significant perturbation of the native structure, despite the fact that this is a bare noble metal surface.

The variation in peak potential with scan rate, characteristic of quasi-reversible electrochemical systems, can be used in the determination of electron transfer rate constants. Specifically, the separation of anodic and cathodic peak potentials (ΔE_p) as the scan rate crosses into a regime where molecular electron transfer characteristics are current-limiting (non-Nernstian behaviour) can be plotted against a logarithmic voltage scan rate. The peak divergence in these "trumpet plots" can be analysed using relations derived by Laviron for chemisorbed electroactive molecules [34]. Briefly, slopes of linear regression fitted to the diverging parts of the

Table 1
The electrochemical characteristics of plastocyanin (a) and azurin (b) molecular monolayers on Au(III)

	$E_{1/2}$ (mV) vs SCE	Surface coverage (10^{-14}) (molecules cm^{-2})	I_{pa}/I_{pc}	ΔE_p (mV)	k_{et} (s^{-1})
PCSS	163 ± 10	2–8.5	1.0–1.2	63–87	5–26
PCWT	109 ± 5	0.3–1.4	1.0–1.2	63–87	
Az WT	150–165	1.7–2.0	1.2	25–85	300–400
Az K27C	150–165	1.8–2.1	1.2–1.4	35–75	210–320
Az S118C	120–160	1.8–2.1	1.1–1.2	15–70	300–570

The half-wave potential, $E_{1/2}$ is defined as $(E_{pa} - E_{pc})/2$.

semi-logarithmic plot can be fitted to: $\log k_{et} = \alpha \log(1-\alpha) + (1-\alpha)\log\alpha - \log(RT/nFV) - \alpha(1-\alpha)nF\Delta E_p/2.3RT$, where α is the electron transfer coefficient (assumed here to have a value of 0.5) and the other terms have their usual meaning. Peak separation observations made with PCSS adlayers (80 mV at a scan rate of 10 mV s^{-1}) were observed to be consistent with quasi-reversible kinetics, and rate constants of 5–25 s^{-1}.

In order to investigate the role of the disulphide bridge introduced, analogous voltammetric investigations were performed with wild-type plastocyanin (PCWT). Though faradaic responses were observed with this protein form, the signals were noticeably broader and weaker than those observed for the immobilised mutant (Fig. 3(c)). Such behaviour is consistent with either lower protein coverage and/or, less robust/more denaturing adsorption. (The PCWT coverage from the peak areas in the CV spectra was estimated to be 7×10^{13} molecules cm^{-2}, lower than that obtained for the PCSS.) Calculated peak widths at half height were ~90 and 115–125 mV for PCSS and PCWT adlayers, respectively. The broader voltammetric peaks observed with the wild-type protein may be reflective of uncontrolled (and accordingly variant) protein surface orientation. In the absence of an anchoring surface group the protein is expected to be physically adsorbed rather than chemically anchored. Regardless of the details, the protein–surface interaction is clearly quite different to that observed with the mutant. The broad voltammetric responses made kinetic determinations with the wild-type protein unfeasible. The negative shift (~50 mV) in half wave potential in comparison with the PCSS form was further consistent with some structural perturbation of the adsorbed wild-type protein.

The surface-cysteine mutant and wild-type azurins display a high affinity for pristine gold electrode surfaces and can be assembled into well-ordered molecular arrays sufficiently robust for high-resolution tunnelling or topographic analyses to be possible under solution (Fig. 4). The tunnelling conductance of a protein under such conditions is such that high contrast can be obtained in constant current imaging. Studies are presently underway to examine, in more depth, the nature and dominant contributing factors to this conductance. Though routinely capable of atomic resolution on crystalline materials, tunnelling imaging of biomolecules is rarely achievable at more than a gross molecular level of resolution. Both (hydrated) molecular compressibility and inherent molecular dynamics are likely to play a significant limiting role in attainable resolution. Reducing the temperature of the sample will restrict both conformational and diffusive motion and may facilitate an increase in imaging resolution. It is known that the Young's modulus of a protein molecule increases by an order of magnitude as the temperature falls below 0 °C; a 'stiffer', more rigid biomolecule is less likely to suffer tip-induced deformation [35,36]. Preliminary low-temperature *fluid* tunnelling analyses of these azurin adlayers have suggested (Fig. 4(b)) that resolution of the bioelectrochemical interface is at least comparable (and often greater) than that attainable at room temperature.

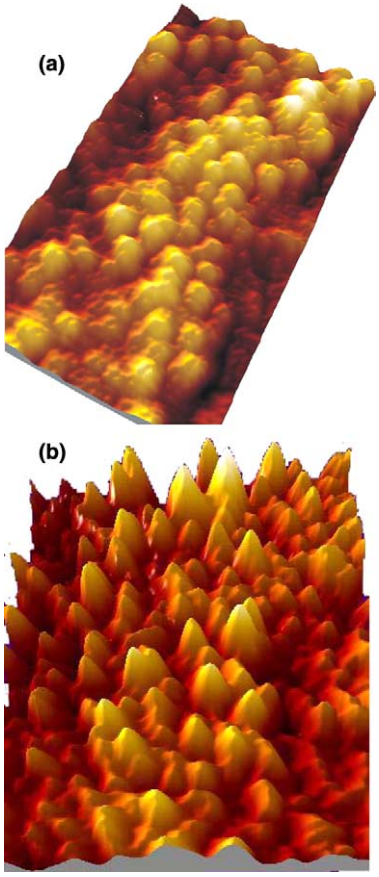

Fig. 4. (a) Fluid tunnelling image (resistance 8.8 GΩ) of a K27C azurin monolayer on Au[III] obtained under a 50:50 water + glycerol solution at room temperature. The substrate had been exposed to 1.3 μM azurin solution overnight. (b) Fluid tunnelling image (8.8 GΩ, 90 × 100 nm) of an azurin monolayer obtained at 0 °C. *Z* scales 0–1.4 nm.

The azurin adlayers all exhibit facile electron transfer to the underlying bare gold electrode surface (Figs. 5 and 6). This is, notably, in contrast to previously reported [14,37] electrochemical analyses of wild-type azurin on gold, in which no faradaic current was detectable by CV and impedance-determined rate constants were determined to be more than one order of magnitude lower than those we report here. The protein coverage, determined by integration of the voltammetric data, was found to be $1.8–2.2 \times 10^{13}$ molecules cm^{-2}. As with plastocyanin, heterogeneous electron transfer rate constants were calculated by monitoring the variation in cyclic voltammetry peak separation with scan rate (Fig. 7) according to the method of Laviron and are summarized in Table 1. Though faster rates of electron transfer have been observed with azurin immobilized on pyrolytic graphite surfaces, these figures are indicative of

facile communication between the copper centres and the underlying bare gold electrode surface. Significantly, however, the rate of electron transfer observed with the S118C protein is not greatly different from that observed with the wild-type protein, despite a greatly reduced copper-electrode separation. In considering the effect of surface mutagenesis on orientation we have assumed that the reactive, solvent-exposed, cysteine residue provides the dominant, directing, means of interaction with the bare gold surface and hence that K27C adopts a surface-bound orientation very similar to that of the wild-type protein, with the S118C mutant bound in an orientation approximately perpendicular to this [38].

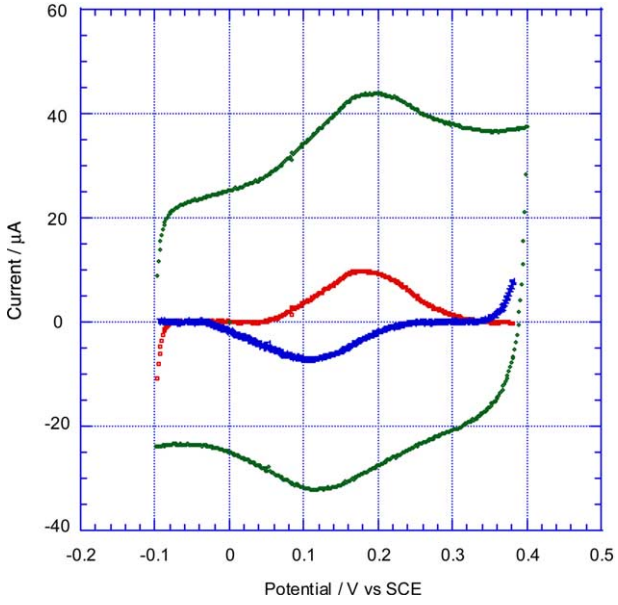

Fig. 5. Voltammetric response (100 mV s^{-1}) of the mass of the azurin adlayer on polycrystalline gold in 100 mM potassium phosphate buffer, pH 7.4. Both raw and background subtracted data sets are shown.

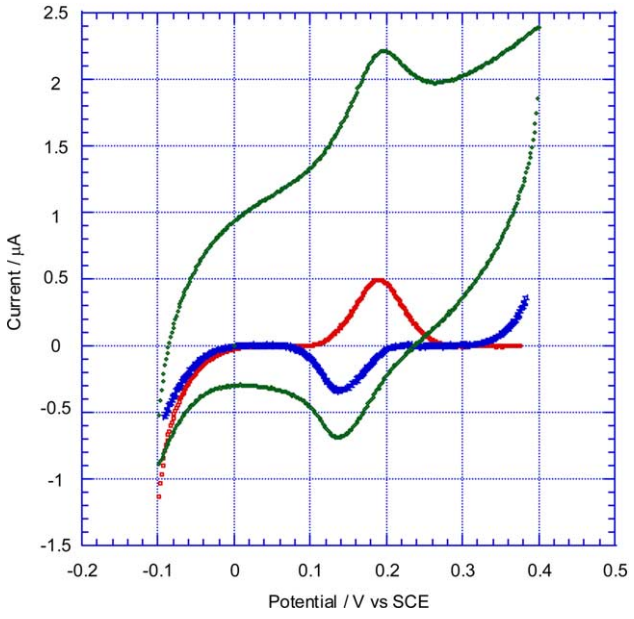

Fig. 6. Voltammetric response (100 mV s^{-1}) of the K27C adlayer on Au[III]. The background subtracted response is also shown.

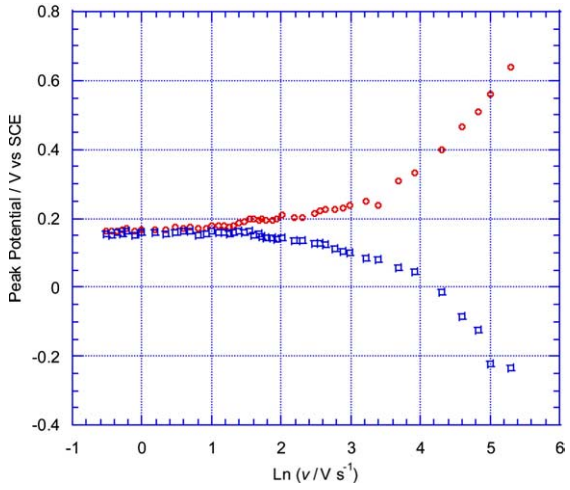

Fig. 7. Anodic and cathodic peak positions (vs SCE) as a function of scan rate (logarithmic scale) of a K27C azurin monolayer on Au[III] evaporated film gold electrode.

A number of studies have shown that the rate of long range electron transfer between metal electrodes and self-assembled electroactive species decreases logarithmically with SAM (self-assembled monolayer) chain length [37,39] and the reaction rate variation can be described by $k_{et} = k_{(n=0)}e^{-\beta n}$ where $k_{(n=0)}$ denotes the rate constant extrapolated to n (number of methylenes) $= 0$. The exponential decay constant, β, has been found, with a number of electrochemical systems, to be 1.0 ± 0.1 Å^{-1} per methylene. To examine further the apparent independence of redox kinetics on copper-gold tunnelling distance in immobilised azurin layers, the mutant proteins were immobilized on (variable thickness) alkanedithiol spacer monolayers (on which one expects the protein bound orientation to be the same as that on bare gold). On such monolayers, one expects immobilisation to occur by dimerisation between the exposed cysteine thiol and the terminal thiol of the SAM. With the wild-type protein, ''reaction'' with such SAMs, if it takes place, must occur with cleavage of its native disulphide moiety. Semi-logarithmic plots ($\ln k_{et}$ vs distance, Fig. 8) revealed reasonable linear correlations from which a distance decay factor β of ~0.2 Å^{-1} was calculated, a value consistent with a minimal distance dependence of the rate of electron transfer. On increasing this spatial separation further by adsorbing the protein onto a C_{12} chain alkanethiol linker the rate of electron transfer was observed to decrease significantly to ~10 s^{-1}. We have concluded that, at close proximity to the electrode surface, i.e., when the protein is anchored directly to gold through its exposed surface cysteine, the electron

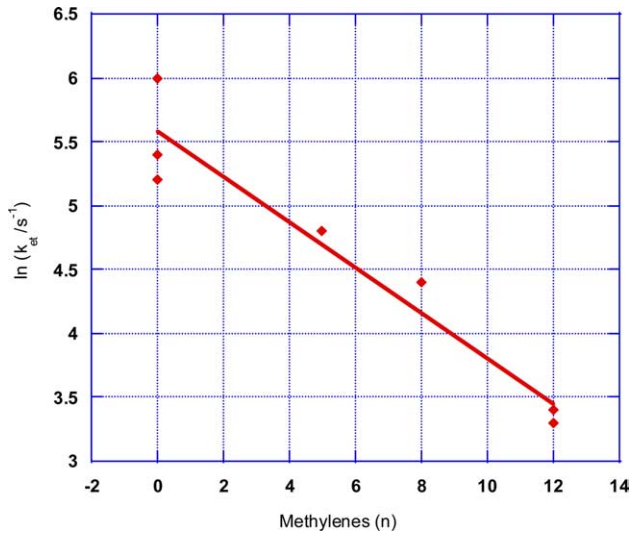

Fig. 8. The dependence of rate of electron transfer between K27C azurin and an underlying gold electrode surface on dithiol linker length. Though there is some scattering of the kinetic data points, they are clearly consistent with a low distance dependence ($\beta \sim 0.2$ Å^{-1}).

transfer kinetics appear to be independent of the copper–gold tunnelling distance, an observation consistent with the presence of a gating process. Such observations have been made before with both cytochrome *c* and azurin [40], and assigned to both preceeding configurational rearrangements associated with achieving molecular orientations in which efficient electron-transfer pathways are most accessible (from surface-bound orientations in which protein–surface interactions are most thermodynamically favourable – since these are not necessarily the same) and electric field effects [41,42]. In the case of the azurin adlayers studied here, we have observed that, on increasing the copper-electrode spatial separation further (>∼12 Å), the tunnelling distance becomes rate-limiting and the rate of electron transfer falls exponentially.

With some adlayers we have observed a 20–40 mV negative shift of the S118C half wave potential. We believe that this is related to the relatively limited solvent exposure of the 118C residue and the mild structural deformation that is known to accompany its covalent binding [43]. Significantly, this perturbation is not evident in data acquired from the other protein forms. Voltammetric peak widths (FWHM) were 60–65, 75–80 and 85–110 mV for the S118C, K27C and wild-type metalloprotein forms, respectively. Since this parameter is diagnostic of electron transfer kinetics and/or homogeneity at the electrode surface [44], and the kinetic differences are minimal (Table 1), these values are consistent with increasing degrees of heterogeneity in the protein monolayers. Predictably, this is greatest with the wild-type protein in which one may expect an appreciable amount of "randomly" physisorbed molecular species to be present.

4. Conclusions

Site-directed mutagenesis methodologies, utilised successfully in the formation of well-defined protein and enzyme adlayers in recent years [11–13,38] have been extended to the blue copper protein, plastocyanin. Robust electrochemical responses, indicative of gross structural retention, at high protein coverage, can be obtained on pristine bare polycrystalline gold electrode surfaces. Observations made during this study, and others, are consistent with the suggestion that the denaturing characteristics of bare metal surfaces can be largely nullified if the protein surface mobility can be restricted (with azurin, the wild-type protein is somewhat unusual in being itself able to chemisorb to gold electrodes). The rate of electron transfer has been found to be largely independent of surface-bound orientation, an observation consistent with the existence of an (as yet undefined) preceeding "gating process". The ability to form functionally active protein/enzyme adlayers on atomically flat single crystalline metal surfaces facilitates experiments in which single molecule (proximal probe based) electronic molecular analyses can be made. Importantly, by anchoring high-purity protein to carefully prepared gold surfaces, rate constants comparable to those observed at gold electrodes modified with saturated adsorbates can be obtained.

Acknowledgements

The authors acknowledge the Engineering and Physical Sciences Research Council (H.A.O.H. and J.J.D.) and the EC SAMBA Project. J.J.D. would also like to thank The Royal Society for financial support.

References

[1] F.A. Armstrong, J. Chem. Soc., Dalton. Trans. 5 (2002) 661.
[2] F.A. Armstrong, H.A. Heering, J. Hirst, Chem. Soc. Rev. 26 (1997) 169.
[3] L.J.C. Jeuken, P. van Vliet, M.P. Verbeet, R. Camba, J.P. McEvoy, F.A. Armstrong, G.W. Canters, J. Am. Chem. Soc. 122 (2000) 12186.
[4] J. Hirst, F.A. Armstrong, Anal. Chem. 70 (1998) 5062.
[5] F.A. Armstrong, H.A.O. Hill, N.J. Walton, Acc. Chem. Res. 21 (1988) 407.
[6] F.A. Armstrong, P.A. Cox, H.A.O. Hill, V.J. Lowe, B.N. Oliver, J. Electroanal. Chem. 217 (1987) 331.
[7] J.E. Frew, H.A.O. Hill, Eur. J. Biochem. 172 (1988) 261.
[8] H.A.O. Hill, Coord. Chem. Rev. 151 (1996) 115.
[9] E.F. Bowden, F.M. Hawkridge, H.N. Blount, J. Electroanal. Chem. 161 (1984) 355.
[10] D.E. Reed, F.M. Hawkridge, Anal. Chem. 59 (1987) 2334.
[11] J.J. Davis, C.M. Halliwell, H.A.O. Hill, G.W. Canters, M.C. van Amsterdam, M.P. Verbeet, New J. Chem. 10 (1998) 1119.
[12] J.J. Davis, D. Djuricic, K.K.W. Lo, E. Wallace, L. Wong, H.A.O. Hill, Faraday Discuss. Roy. Soc. 116 (2000) 15.

[13] J.J. Davis, H.A.O. Hill, J. Chem. Soc., Chem. Commun. 5 (2002) 393.
[14] Q. Chi, J.D. Zhang, J.U. Nielsen, E.P. Friis, I. Chorkendorff, G.W. Canters, J.E.T. Andersen, J. Ulstrup, J. Am. Chem. Soc. 122 (2000) 4047.
[15] P. Facci, D. Alliata, S. Cannistraro, Ultramicroscopy 89 (2001) 291.
[16] W. Haehnel, Ann. Rev. Plant Physiol. 35 (1984) 659.
[17] J.M. Guss, P.R. Harrowell, M. Murata, V.A. Norris, H.C. Freeman, J. Mol. Biol. 192 (1986) 361.
[18] J. Han, E.T. Adman, T. Beppu, R. Codd, H.C. Freeman, L. Huq, T.M. Loehr, J. Sanders-Loehr, Biochemistry 30 (1991) 10904.
[19] J.M. Moore, C.A. Lepre, G.P. Gippert, W.J. Chazin, D.A. Case, P.E. Wright, J. Mol. Biol. 221 (1991) 533.
[20] P.C. Driscoll, H.A.O. Hill, C. Redfield, Eur. J. Biochem. 170 (1987) 279.
[21] S. Bagby, D. Phil. Thesis, University of Oxford, 1991.
[22] E. Vakoufari, K.S. Wilson, K. Petratos, FEBS Lett. 347 (1994) 203.
[23] R.J.P. Williams, Eur. J. Biochem. 234 (1995) 363.
[24] M.D. Scawen, J.A. Ramshaw, D. Boulter, Biochem. J. 147 (1975) 343.
[25] M.R. Redinbo, T.O. Yeates, S. Merchant, J. Bioenerg. Biomembr. 26 (1994) 49.
[26] K. Sigfridsson, S. Young, O. Hansson, Eur. J. Biochem. 245 (1997) 805.
[27] L. Andolfi, S. Cannistraro, G.W. Canters, P. Facci, A.G. Ficca, I.M.C. van Amsterdam, M.Ph. Verbeet, Arch. Biochem. Biophys. 399 (2002) 81.
[28] L. Andolfi, S. Cannistraro, G.W. Canters, J.J. Davis, M.Ph. Verbeet, H.A.O. Hill, submitted for publication.
[29] H. Nar, A. Messerschmidt, R. Huber, M. van de Kamp, G.W. Canters, J. Mol. Biol. 221 (1991) 765.
[30] I.M.C. van Amsterdam, M. Ubbink, L.J.C. Jeuken, M.Ph. Verbeet, O. Einsle, A. Messershmidt, G.W. Canters, Chem. Eur. J. 7 (2001) 2398.
[31] F.A. Armstrong, A.M. Bond, H.A.O. Hill, B.N. Oliver, I.S.M. Psalti, J. Am. Chem. Soc. 111 (1989) 9185.
[32] L.S. Conrad, H.A.O. Hill, N.I. Hunt, J. Ulstrup, J. Electroanal. Chem. 364 (1994) 17.
[33] D.D.N. McLeod, H.C. Freeman, I. Harvey, P.A. Lay, A.M. Bond, Inorg. Chem. 35 (1996) 7156.
[34] E. Laviron, J. Electroanal. Chem. 101 (1979) 19.
[35] Y. Zhang, S. Sheng, Z. Shao, Biophys. J. 71 (1996) 2168.
[36] C.B. Prater, M.R. Wilson, J. Garnaes, J. Massie, V.B. Elings, P.K. Hansma, J. Vac. Sci. Technol. B 9 (1991) 989.
[37] Q. Chi, J.D. Zhang, E.P. Friis, E.P. Andersen, J.E.T. Ulstrup, J. Electrochem. Commun. 1 (1999) 91.
[38] J.J. Davis, D. Bruce, G.W. Canters, J. Crozier, H.A.O. Hill, J. Chem. Soc., Chem. Comm. 5 (2003) 576.
[39] A.M. Becka, C.J. Miller, J. Phys. Chem. 96 (1992) 2657.
[40] H.O. Finklea, L. Liu, M.S. Ravenscroft, S. Punturi, J. Phys. Chem. 100 (1996) 18852.
[41] A. Avila, B.W. Gregory, K. Niki, T.M. Cotton, J. Phys. Chem. B 104 (2000) 2759.
[42] D.H. Murgida, P. Hildebrandt, J. Am. Chem. Soc. 123 (2001) 4062.
[43] I.M.C. van Amsterdam, M. Ubbink, G.W. Canters, Inorg. Chim. Acta 331 (2002) 296.
[44] A. Bard, L. Faulkner, Electrochemical Methods: Fundamentals and Applications, Wiley, New York, 1980.